Journal of Statistical Physics, Vol. 70, Nos. 1/2, 1993

Brain Stem Neuronal Noise and Neocortical "Resonance"

Arnold J. Mandell[1] **and Karen A. Selz**[1]

We present a qualitative model and data in evidence for the selection and stabilization of neocortical brain-wave power spectral modes by slow periodic and fast noise driving by brain stem neurons. Unlike noise effects in a bistable potential, increasing noise amplitude via more brain stem neurons increases the measure on unstable manifolds trapped in the saddle-sinks of the neural membrane attractor and *increases* dwell times. We suggest that the effect of noise in expanding dynamical systems such as the generalized neuronal membrane equations studied here may be analogous to that of many-frequency quasiperiodic driving which leads to the stabilization of the EEG as a strange, nonchaotic attractor.

KEY WORDS: Brain waves; neurons; stochastic resonance; strange nonchaotic attractor; quasiperiodic driving; noise.

1. INTRODUCTION

Using ergodic dynamical measures, (the growth rate of the longest) run statistics, and the higher moments of probability density distributions, we have been able to discriminate among the patterns of individually recorded, interspike interval sequences of four neuroanatomically and neurochemically distinct brain stem neuron types.[1] Due to the irregularity and average frequency ranges of their interspike interval patterns and the diffuseness of the distribution and influence of their axonal endings throughout the brain, these (and additional brain stem cell types to be discussed here) can be viewed as roughly analogous to "noise sources" modulating global brain dynamics.[2]

[1] Laboratory of Experimental and Constructive Mathematics, Departments of Mathematics and Psychology, Florida Atlantic University, Boca Raton, Florida 33431.

822/70/1-2-23

0022-4715/93/0100-0355$07.00/0 © 1993 Plenum Publishing Corporation

Of interest here is how these brain stem noise systems regulate the dynamics of neocortical pyramidal cells responsible for the brain wave patterns (electrovoltage potential variations with time, recorded from the surface of the brain or scalp and reference site) which are closely associated with and help define levels of consciousness, including sleeping, waking, dreaming, relaxing, attending, and excited states.[3,4] Recent applications of a model involving noise-induced information transport in a nonlinear, bistable, weakly periodically driven, simple sensory nerve system[5,6] suggest attempts at generalization to more realistically complicated multimodal integrative brain functions. Although neuronal representation via a bistable potential is apparently relevant to peripheral and central brain sensory mapping systems, even a two-neuron, negatively and positively, self- and other coupled, nonlinear system can (like much larger real neuronal networks) express the variety of dynamics that are known to exist in invertible and noninvertible diffeomorphisms of the plane.[7]

The role of brain stem noise "irregularity" in the selection and temporary stabilization of the "regularity" in brain wave modes and states of consciousness has been a long-standing problem in behavioral neuroscience.[8] Electrolytic destruction in these brain stem systems generates a comatose state in the experimental aniimal without arousability through any form of sensory stimulation. However, coma can be temporarily reversed into a variety of "higher levels of consciousness" dependent upon the frequency, wave form, and amplitude of the electrical stimulation through electrodes placed in front of the lesion.

The loss of brain stem and related diffusely projecting neuronal cell systems in humans is associated with deficits in what are called "fundamental functions" such as maintenance of attention, concentration, sleep, arousal, motivation, and accuracy and rate of information processing, all in a class of neurological syndromes called the subcortical dementias.[9]

Changes in brain function with age and their potential for retardation or reversal can be approached within the context of stochastic-like, brain stem neuronal dynamics.[10]

2. DWELL TIMES IN NEURONAL MEMBRANE SADDLE-SINKS

Interspike interval patterns in some sensory systems in response to weak periodic stimulation demonstrate exponentially decaying dwell-time density distributions $\rho(\tau)$ peaked at all or odd-integer multiples of the amplitude (m), frequency (ωt), (weak) driving with $m \sin(\omega t)$ in the presence of (assumed) delta-correlated (or colored) noise $\xi(t)$, much like

those observed in simulations of Langevin-like equations representing a bistable potential of the general form $dx/dt = x - x^3 + m\sin(\omega t) + \xi(t)$.[5,6]

Although two-state, "all-or-none" neuronal activation patterns have a distinguished history in theories of neuronal information transport,[11] and modern patch-clamp theory approaches the issues of neural membrane channel conductances as a Markov statistical problem in "open versus closed," two-state dynamics,[12] evidence is emerging that even "molecular" ion channel dynamics involve multiple characteristic times that scale "fractally,"[13,14] that is, $\rho(\tau) \cong \exp(-kt^{\beta})$, $0 \leqslant \beta \leqslant 1$, suggesting attractors of the neural membrane dynamics that are more complicated than one-dimensional anharmonic potentials with periodic forcing, damping, and noise.

Intermittency (irregular alterations between near periodic and aperiodic recurrent behavior), characteristic of systems near inverse saddle node bifurcations and homoclinic tangencies, is seen as "bursting" patterns in time series of neuronal firing and the episodic waxing and waning of brain-wave amplitude–frequency relations called spindle bursts. These behaviors are more typical than the n-periodic interspike interval patterns of classical stochastic resonance.[15,16]

The brain stem neuronal noise sources to the brain-wave nonlinear oscillators range in frequency from 0.5 to >130 Hz, with two or more characteristic (average) frequencies. These are transmitted "upward" via axons, sometimes projecting from neighboring cells in the same nuclei in the lower brain to the same regions in the neocortex, suggesting the phrase "quasiperiodic noise driving of the neocortex."[17]

A qualitatively realistic representation of the time dynamics of neural membranes, single neurons, and "global" brain-wave-generating neural membranes, then, is a generic, nonautonomous, highly nonlinear relaxation oscillator with parameter values such that recurrent orbits visit critical point regions on the (vertical) slow manifold of phase space which are subject to an attractive–repulsive conflict ("saddle-sinks")[18] between faster neural activation potential "spike" transitions on the (horizontal) fast-manifold to the next saddle-sink. Noise-amplitude-sensitive density distributions of regional (s) "dwell times" $\rho_s(\tau)$ results.

Neurophysiologically, $\rho_s(\tau)$ reflects preactivation refractoriness to excitation, including repolarization–depolarization processes subject to subtle neurochemical and metabolic influences (e.g., sensitization and habituation) over longer time scales and otherwise apparently adiabatically removed from the time series of observables.[20] With the inclusion of these longer time scales, a membrane in a state of excitation will be more likely to output bursts (instead of single discharges) in response to perturbation.

If it exists, an invariant probability measure representing (up to a

renormalization of time) the frequency and duration with which regions in phase space are visited over the time evolution of a dynamical system is a physical, natural measure; on uniformly hyperbolic (divergent), exponentially mixing attractors, this is known as the Sinai–Ruelle–Bowen (SRB) measure.[19] In nonuniformly hyperbolic systems, such as the ones reported here, little is known, such that measures such as $\rho_s(\tau)$ are made empirically from numerical and real experiments. We will focus on nonnormalized observables directly using a histogram of phase-space regional dwell times, $h_s(\tau)$.

The model with relevance to both the membrane dynamics of a single neuron and the global membrane dynamics of brain waves[21,16] is the prototypic nonautonomous van der Pol relaxation oscillator[18] with noise, which we study on an EAI-680 analog computer as

$$\frac{d^2x}{dt^2} = -r(x^2-1)\frac{dx}{dt} - x + \omega r\beta\cos(\omega t) + \alpha f(t)$$

with $r = 21.5$, $\beta = 205$, $\omega = 0.6$ Hz, and $f(t)$ is colored noise at 60 Hz with noise amplitude α, being the parameter of interest.

The rather contrived values for r and β resulted from searches for parameter regions where relatively stable multiple preloop toroidal "wrinkles" could be observed. This prechaotic state lives near homoclinic tangencies between stable (W^s) and unstable (W^u) manifolds in which small amounts of noise can be dynamically decisive. The two orders of magnitude difference between ω and $f(t)$ simulates the relative range of the slow periodic driving and fast noise dorsal raphe-hippocampal cortex brain-stem neuronal driving systems (data from Kocsis and Vertes, 1992, in preparation) discussed below. In addition, the very slow periodic driving term ω has validity with respect to the differential system in light of the fact that output frequencies can be as much as 400 times the input frequencies[22] and, as in any nonlinear system, not necessarily harmonic.

Using the method of matched asymptotic expansions and partitioning the saddle-sink region into four different relatively homogeneous areas (s_{1-4}, s_1 being the subregion of slowest orbital transit), Grasman *et al.*[22] found that without $\alpha\xi(t)$, the system in s_1 required rescaling with respect to *two independent time dependences:* the dwell time within each subregion (a function of r and β) and the inverse frequency within it [dependent on $\cos(\omega t)$ and β] in order to obtain solutions. Our addition of colored noise results in *a third independent time dependence* involving $\alpha\xi(t)$ with respect to the distribution of saddle-sink dwell times $h_{s_i}(\tau)$, and this along with the large nonlinearity and multiplicity of extrinsic times required numerical simulation for even qualitative explication.

Figure 1 portrays representative results comparing the changes in the

geometry of the x versus dx/dt phase plots with their associated h_{s_1} in the boxed saddle-sink region, including Grasman's subregion of longest orbital transit time.[22] These two symmetric regions in phase space have been called *saddle-sinks* because they represent a region of intersection of the annular contraction onto the vertical slow manifolds from inside and out-

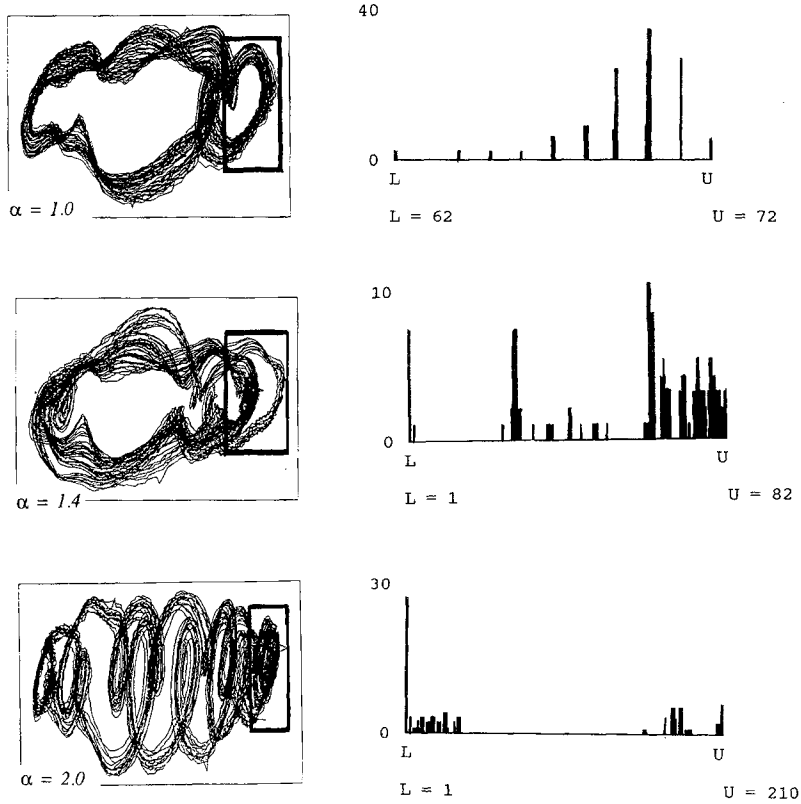

Fig. 1. Noise amplitude changes the pattern of dwell times in the saddle-sink region of the global neural membrane model. Phase portraits of the digital reconstructions of an EAI-680 analog computer simulation of the highly nonlinear, periodically driven, van der Pol equations over the indicated increases in the noise amplitude term α (see text for the equation and the parameter values). The saddle-sink areas (Grasman area s_1) studied with dwell time histograms are indicated by the boxes. With increasing α, qualitative changes in the phase portrait from multiple folds ("wrinkles") to smooth loops are observed associated with transitions from dwell time distributions with a single average, to a multimodal pattern, to a bimodal combination of short and long times. Stretching the unstable, slow, vertical, manifolds trapped in the saddle-sinks is postulated to be the global topological mechanism for the observed increase in dwell times with noise.

side the recurrent orbit bundle (i.e., actions along the stable manifold, W^s) and divergence in an up-and-down shuffling motion vertically along it (i.e., actions along the unstable manifold, W^u). This can be seen to be analogous to the topological arrangement of orbits at a saddle node, $W^u \cap W^s$, but here the contracting action W^s is the dominant one, thus the addition of the word "sink."[18]

In over 40 analog computer experiments (the smooth record digitized at 1 kHz for studies of the relative h_{s_1}) in the parameter neighborhood indicated above, only these three general patterns of h_{s_1} were observed in relationship to the degree of dominance of "wrinkles" versus "loops" in the attractors: (1) Top graphs ($\alpha = 1.0$): a continuous h_{s_1} with an obvious average value which is associated with an orbital geometry characterized by a one-orbital bundle into and out of a singular "wrinkle"; (2) middle graphs ($\alpha = 1.4$): a h_{s_1} reflecting multiple routes through the phase space box containing both wrinkles and loops of the attractor, suggesting three clusters of values (short, medium, and relatively long); (3) bottom graphs ($\alpha = 2.0$) with an h_{s_1} signature of bursting intermittency, a mix of long and short dwell times associated with a geometry dominated by overlapping loops with fast and slow transit times through the saddle-sink region.

Generally, we have found that *increasing the noise amplitude parameter* α *increases both the length and the density of the longest dwell times in the saddle sink.* This is clear in the h_{s_1} of Fig. 1. This finding is in contrast to what we might expect for noise amplitude and switching time in a bistable potential.

The three h_{s_1} patterns of Fig. 1 are more characteristic of interspike interval (ISI) histograms of brain stem neuronal systems[23,24] than the distribution of odd or all-integer, n-periodic ISI of stochastic resonance.[5,6] In the context of the global membrane equations of neocortical brain waves, these three patterns of h_{s_1} are analogous to the single dominant mode, multiple mode, and "spindle burst" electroencephalographic patterns common to human and animal recordings.[25] Consonant with the mechanisms of a more generalized idea of stochastic resonance, noise amplitude is serving the function of selection and stabilization of ISI brain wave relevant h_{s_1}.

3. A TOPOLOGICAL MECHANISM FOR INCREASES IN SADDLE-SINK DWELL TIMES: STRETCHING THE SRB MEASURE ON W^u

Attracting sets like those in Fig. 1 tend to be unions of W^u. The W^s can be said to "iron down" the orbits along the stretching directions of the attractor composed of $\bigcup W^u$. As noted in Fig. 1, the saddle-sink regions

studied with respect to h_{s_1} are those in which the foliations of W^u are "trapped" between those of W^s. The SRB measure (when constructable) measures the time spent (i.e., densities of the orbits) in regions in phase space, and would then be some approximation of a smooth measure on the attractor along the stretching, unstable direction W^u. A small amount of stochastic perturbation $\alpha f(t)$ would be expected to increase the measure of W^u beyond that of the dynamical system without noise, and influenced by the deterministic vectorial direction fields, appear to stretch the occupied region further.[26–28]

That is, additive noise increases the density of points "trapped" on W^u in the saddle-sink and increases the densities and sizes of the longest dwell times in h_{s_1}. This idea is consistent with the results of numerical simulations graphed in Fig. 1. The effect amounts to something beyond stochastic stability with respect to saddle-sink dwell times, and serves as one source of a theory for explaining how brain stem neuronal noise has (for many decades) been observed to make the perceptual, motor, and cognitive functions attributed to the neocortex more coherent.[29]

To demonstrate the noise-induced W^u stretching directly, Fig. 2 represents the results of a numerical study of a discrete van der Pol map driven by a period seven (specifically, $\lambda = 3.701769$) of the Metropolis–Stein–Stein periodic orbits of the logistic map $[f(\omega) = \lambda(\omega - \omega^2)]$,[16] plus δ-correlated equiprobable noise $\alpha f(t)$. Results are graphed from numerical studies in a homoclinic-near-tangency-like parameter region, in a "bubble" neighborhood ($r = 1.963$–1.964, $\beta = 0.315$) (top left) of "antimonoticity,"[30] that is, in a region of parameter space where there is simultaneous creation and destruction of periodic orbits across increasing parameter r, in a regime analogous to that of the wrinkled torus studied in the continuous case (see Fig. 1). The system is

$$x_{t+1} = y_t - r\left(x_t - \frac{x_t^3}{3}\right)$$

$$y_{t+1} = -\frac{x_t}{r} + r\beta\cos(\omega t) + \alpha f(t)$$

with the source of ω for each time step as indicated above.

Figure 2 demonstrates that increasing the noise amplitude term α in the discrete map results in smoothing and stretching of the period-7 doubled point set along W^u postulated to be the mechanism of noise-amplitude-increased saddle-sink dwell-time length in the smooth attractor. The (unseen) vector field of W^s compresses and smooths the noise down onto W^u, which, in turn, stretches it.[26] Measures that are continuous along unstable directions, the (combination of) SRB measures on the

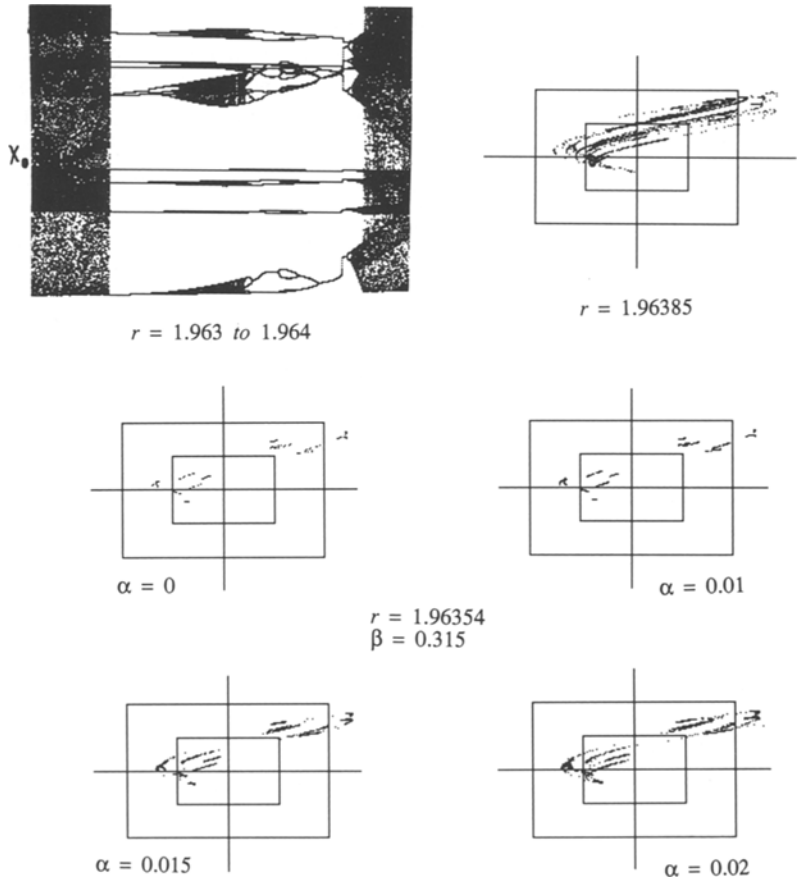

Fig. 2. Noise amplitude stretches the unstable manifolds of a discrete, periodically-driven van der Pol expanding attractor, the topological mechanism postulated to be responsible for the increases in the longest dwell times observed across increasing noise amplitude in Fig. 1. The results of studies of a discrete van der Pol-like map driven by the quadratic map of the unit interval at a parameter value of 3.701769 (a period seven) with additive δ-correlated equidistributed noise. The system was studied in a near homoclinic tangency regime, a Yorke "bubble" of creation and destruction of periodic orbits seen in the bifurcation plot in the upper left (see text for the equation, parameter values, and interpretation).

pieces of $W^{u,(27,28)}$ are then increased with increasing noise amplitude α. Figure 2 serves as one explanation for the results in Fig. 1, though, of course, unlike the continuity of stretching-induced wrinkles and loops in the smooth system, a discrete map generates points which jump discontinuously among the pieces of W^u, such that computations of h_{s_1} in any small box in this system is without the same meaning as those made on the continuous system.

It can be said more generally that the asymptotic SRB measure of an attracting set of an expanding dynamical system is selected by the noise $\alpha f(t)$ {here $f(t)$ is δ-correlated, equiprobable noise on $[0, 1]$} as $\alpha \to 0$. A simple example is the Feigenbaum nonchaotic fractal set at the 2^n period-doubling accumulation point of $f(x) = rx(1-x) + \alpha f(t)$, $r = 3.56995$, seen in Fig. 3 for $\alpha = 0$, 0.001, and 0.1. The locations of neighboring, 2^n periodic repelling points are outlined by the empty intervals of the histogram as $\alpha \to 0$.

As the converse, the condition that the limit set not be zero as $\alpha \to 0$ has been used as a definition of an attractor of a dynamical system.[31] It is from the standpoint of noise selection and stabilization of the limit sets of (nonlinear) expanding dynamical systems[32] that we view brain stem neuronal noise regulation of neocortical electrophysiology and function.[3,4,16]

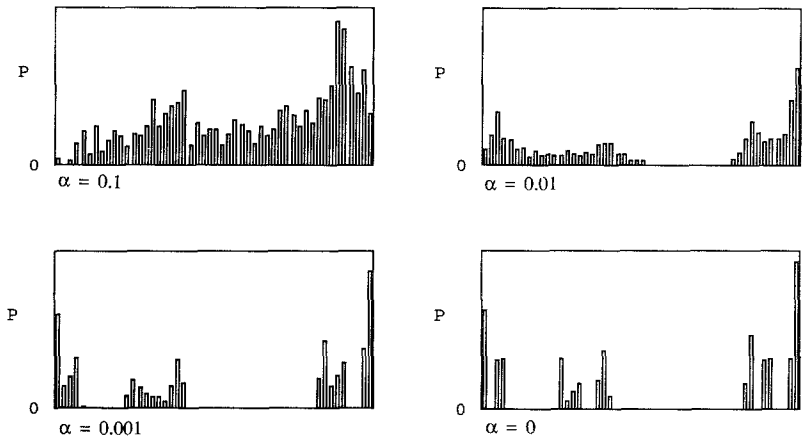

Fig. 3. As in Fig. 2, an example of the selection of the invariant measure in an expanding attractor by δ-correlated equiprobable noise amplitude as $\alpha \to 0$; the quadradic map of the unit interval at a parameter value of 3.56995, the fractal, nonchaotic set at the period doubling accumulation point. We conjecture that this noise effect may be analogous to that of the 2- and 3-frequency quasiperiodic driving stabilization of toroidal strange, nonchaotic attractors (see text for references) and may serve as a metaphor for the way brain stem noise selects and stabilizes power spectral broadband modes of the global neural membrane dynamics of brain waves.

4. THE BRAIN WAVE BROADBAND MODES AS NOISY, STRANGE, NONCHAOTIC LIMIT SETS

There has been a considerable amount of unresolved debate about the neural origins and physiological significance of the electroencephalographic (EEG) measurements of time-dependent microvoltage potential variations as recorded from electrodes placed on the neocortex and scalp. In spite of this, there is a remarkable consistency in the reports of the characteristic power spectral broadband modes that can be observed and their relative dominance in operationally defined states of consciousness.[25,29,33,34]

Described characteristically in the frequency domain and with Greek letter labels, the dominant broadband power spectral modes of the EEG and their associated states are: $\Delta \cong 3$ Hz, deep sleep or coma; $\theta \cong 6$ Hz, light sleep or day dreaming; $\alpha \cong 12$ Hz, relaxed, eyes closed, awake; $\beta \cong 25$ Hz, aroused, very alert, and excited; and $\gamma \cong 35$–50 Hz, regional evidence of very focused attention; 100- and even 200-Hz records have also been reported.[34] Of course, in the time domain, one could describe these modes as a period-doubling progression in seconds: 0.33, 0.166, 0.083, 0.04, 0.02, 0.01,.... This period doubling can be seen along with period adding in parameter regions near torus breakdown through wrinkling.

It is productive to think about the EEG power spectral broadband modes in the context of the period-doubling scenario since it is known that increasing brain stem noise selects the fastest of the broadband frequencies (β and γ) (i.e., the shortest times) in the EEG.[25,29,33,34] It is also well established that additive δ-correlated white noise selectively destroys the longest periods of the period-doubling sequences with increasing noise amplitude in cubic nonlinear differential equations similar to the neural membrane equations studied in Fig. 1.[35]

With functional, chemical, or anatomical impairment of brain stem neuronal noise influences on the EEG, the smallest frequencies (i.e., longest characteristic periods) come to dominate the record. These relatively stationary "slow-wave" states are associated with various degrees of impairment of consciousness, including episodes of automatic behavior (i.e., behavior without apparent awareness or memory for the event) and nonresponsiveness to strong sensory stimuli. Typical records for representative syndromes are graphed in Fig. 4.

These records demonstrate a particular kind of reduced complexity. *Their statistical dynamical characteristics are more stationary than in the normal condition.* This *abnormal stationarity in brain states that are inconsistent with normal awake attentional brain function* has led research groups more interested in measure-theoretic stability than in brain physiology to use cases of unusual EEG alpha stability,[25,36] epilepsy,[37] sleep states,[38]

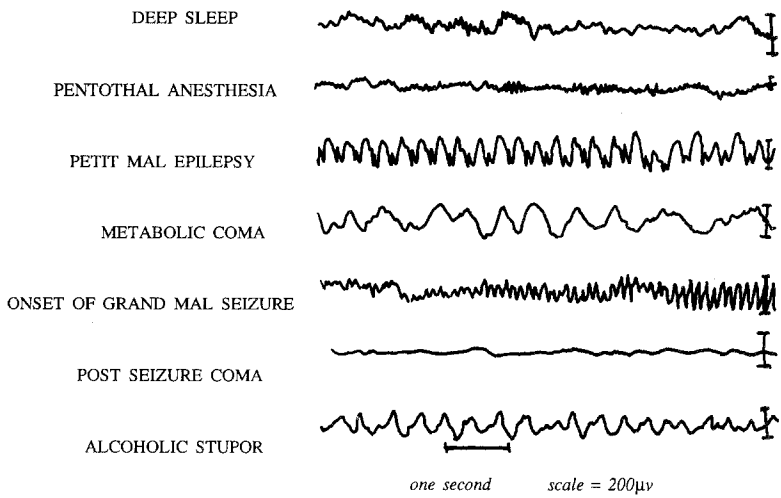

Fig. 4. Example of mostly pathological stationarity in electroencephalographic recordings of brain waves, microvolts (vertical scale) over time. This persistence in statistical patterns of variation in the EEG is not compatible with awake, alert consciousness, which demonstrates normal fluctuations at many time scales. These EEG patterns and their associated states are related to loss of sensitivity to or sources of brain stem noise driving of the neocortex.

or patients with hereditary brain degenerative disorders who are in coma[39] as sources of data for making complexity measures, techniques which are then applied to a normal awake, nonstationary population.

Discriminations between the kinds of records seen in Fig. 4 and normal awake states as in Fig. 5 can be made quite consistently by clinical neurologists through qualitative comparisons. On the other hand, efforts to deal with *normal*, nonstationary brain wave data sets with measures of dimension, expansivity, and entropies have led to much hand-wringing debate,[40] since the measures range widely in the same individuals (as they must, given our states of continually varying attention), and do not speak for themselves with respect to their mechanistic meaning, and because the research that spawns them is not driven by theoretical mathematical hypotheses, the faint hints that may be in the data are readily overlooked.

Another reason to consider a noisy fractal attractor hypothesis for the character of the global brain wave dynamical system is that while evidence suggests that the global dynamic is an attractor and studies are consistent with respect to its being a fractal set, *not one study has proven it to be sensitive to initial conditions convincingly.* Such dynamical structures have been named *strange, nonchaotic attractors.*[41]

The definitional diagnostic triad for this dynamical state, then, is[42,43]: (1) a noninteger, Hausdorff-derived, "dimensional" measure D on the

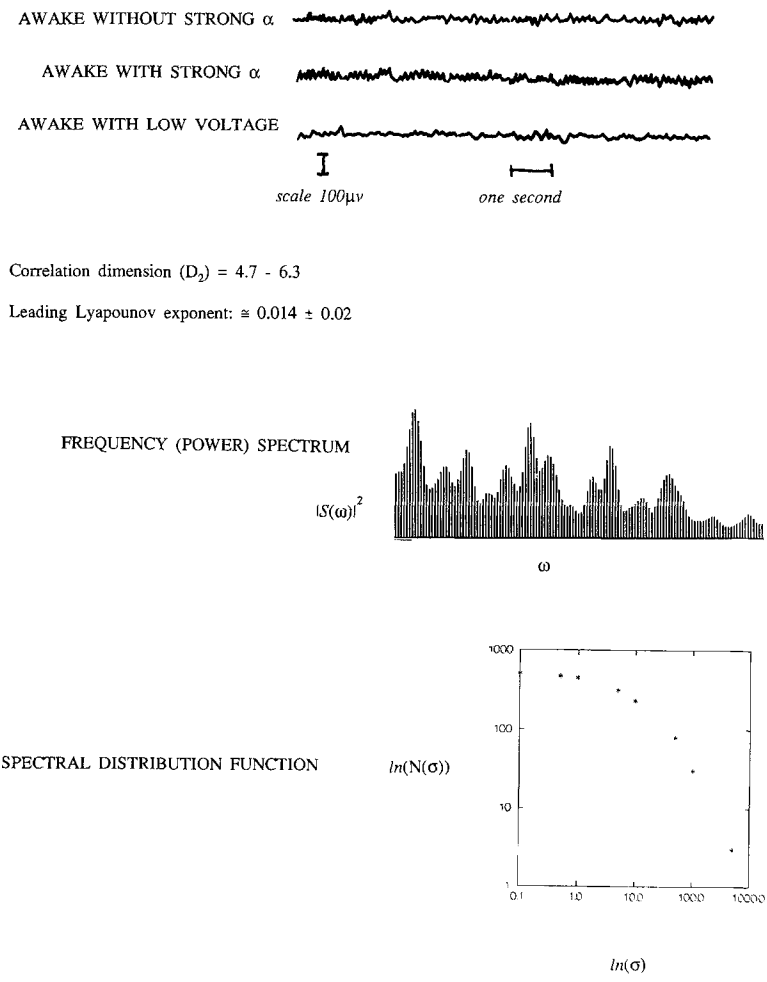

Fig. 5. Measures addressing the question (unresolved): is the EEG a strange, nonchaotic attractor? These records are examples of normal, relaxed, awake brain wave patterns recorded from the midline of the head with varying amounts of α wave (10–12 Hz) dominance. The "fractal" correlation dimension on such records varies as indicated; the leading Lyapunov exponent is characteristically very low positive with large fluctuations (nonuniformity); the power law scaling of power spectral amplitudes, the $N(\sigma)$ plot, falls short of the criteria for a strange, nonchaotic attractor. See text for explication and references (data of Wally Prichard).

phase portrait or Poincaré section of the attractor, generally, for a compact set M and decimation ε,

$$\dim_M = \lim_{\varepsilon \to 0} \sup \ln\{N(\varepsilon)\}/\ln(\varepsilon)$$

(2) evidence for nonexpansiveness of the dynamics (in the mean), an estimate of the sensitivity to initial conditions in the general form of an exponential coefficient, the Lyapunov exponent,

$$\bar{\lambda} = \lim_{n \to \infty} 1/n \ln |d_x f^n \delta x|$$

in which d_x is an estimate of the derivative with respect to x or, in higher dimension, the Jacobian matrix at x, f is the function being evaluated, and δx is a small perturbation or distance between orbits in the neighborhood of x; (3) scaling properties of the Fourier amplitude spectrum of the discrete Fourier transform of the time series of observables which characteristically have many peaks reflecting "wrinkled," sharp corners in the attractor. A useful measure of this property was found to be the spectral distribution function as the number of peaks, $N(\sigma)$, in the Fourier amplitude spectrum with amplitudes $>\sigma$, which in a strange, nonchaotic attractor scales like $N(\sigma) \cong \sigma^{-\eta}$, $1 < \eta < 2$.[42,43]

Using the Wolf algorithm[44] for the computation of the average divergence rate of nearby initial conditions, the Lyapunov characteristic exponent $\bar{\lambda}$ (with a lag of five time steps Δt, $5\Delta t$ intervals between reinitialization, six-dimensional embedding, and normalized to the interval $[0, 2]$), we found that values for the Pritchard data studied did not differ significantly from zero (see Fig. 5). The relatively high variance for these computations reflects (depending upon investigator orientation and bias) either the nonuniformity of expansion rates or the nonstationarity of the signal. Both reflect the reality of the neurophysiological correlates of these normally varying states of consciousness.

Correlation dimension computations, D_2, using a variety of embedding criteria and algorithms[45] lead to fractional values ranging from 4.5 to 6.5 in awake states as in Fig. 5, with the records from some neocortical regions failing to converge.

The $\ln N(\sigma)$ versus $\ln \sigma$ spectral distribution plot in Fig. 5 is indecisive with respect to discriminating strange nonchaotic from strange chaotic attractors,[46] with the left side of the function reflecting a power law of $\eta < 1$ and the right side, $1 < \eta < 2$. Truncating the function as others have done[43,46] would lead in the direction of the latter.

Of interest with respect to the issue of *strange nonchaotic attractors* and the representativeness of the attractor of Fig. 1 is the Rapp brain-wave

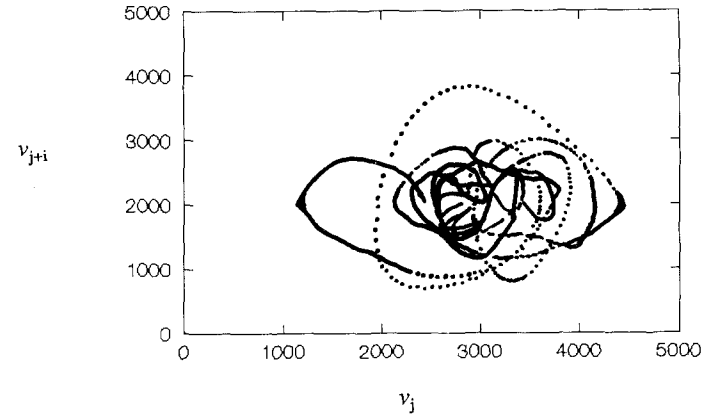

Fig. 6. Thickened folds in a phase portrait of a two-dimensional projection of an eight-dimensional embedding of an EEG record from a relaxed awake subject after the record was reduced to its relevant topological manifold by singular value decomposition. The Rapp awake attractor has a qualitative similarity, with respect to these features, with the model portrayed in Fig. 1. See text for references.

phase-space attractor[45] from waking brain wave records. The EEG time series is projected into $\mathbb{R}^2$ following a suitably lagged embedding in eight-dimensional space after singular value decomposition (equivalent to a reduction to a topological manifold[47]) and orthogonal rotation. Its "thickened" and near singular turning points (Fig. 6) suggest the wrinkles of our model at the strange nonchaotic border of chaos as in Fig. 1.

5. SIMULTANEOUS SLOW PERIODIC AND FAST NOISE DRIVING OF THE SAME NEOCORTICAL REGION BY NEIGHBORING BRAIN STEM CELLS

Consistent with the brain-stem, neuronal noise-regulated, neocortical brain-wave model of the EEG-defined states of consciousness as depicted in Fig. 1, a physiologically significant example of the anatomical juxtaposition of sources of slow periodic and fast noise driving of the same neocortical areas has been demonstrated in the dorsal raphe nucleus of the (mesencephalic) brain stem.[48,49] Figure 7 portrays the shapes of the interspike interval density distributions, their "coherence" in plots of predicted versus observed values of polynomial fits with a five-interspike-interval lag, and the phase portrait of the two cells, each embedded in three dimensions. The differences between the time scales of the cell types range from two to three orders of magnitude, as do those in the model.

Simultaneous recordings of a fast frequency noise cell and hippo-

campal brain waves (Kocsis and Vertes, in preparation) demonstrate that differences in the (auto)correlation time without changes in the mean interspike interval of dorsal raphe fast noise cells are associated with a change in the pattern of power spectral peaks of the hippocampal EEG (Fig. 8).

We have not noted the digitization, sample length, and frequency details in either plot, in that their geometries are sufficiently meaningful in this context, and we would be unable to provide a meaningful account of these details without sufficient development, for which there is insufficient room here. We have treated both states identically.

We would conjecture that a strange, nonchaotic attractor, dwell-time, autocorrelation-as-distribution model is relevant at both the level of the

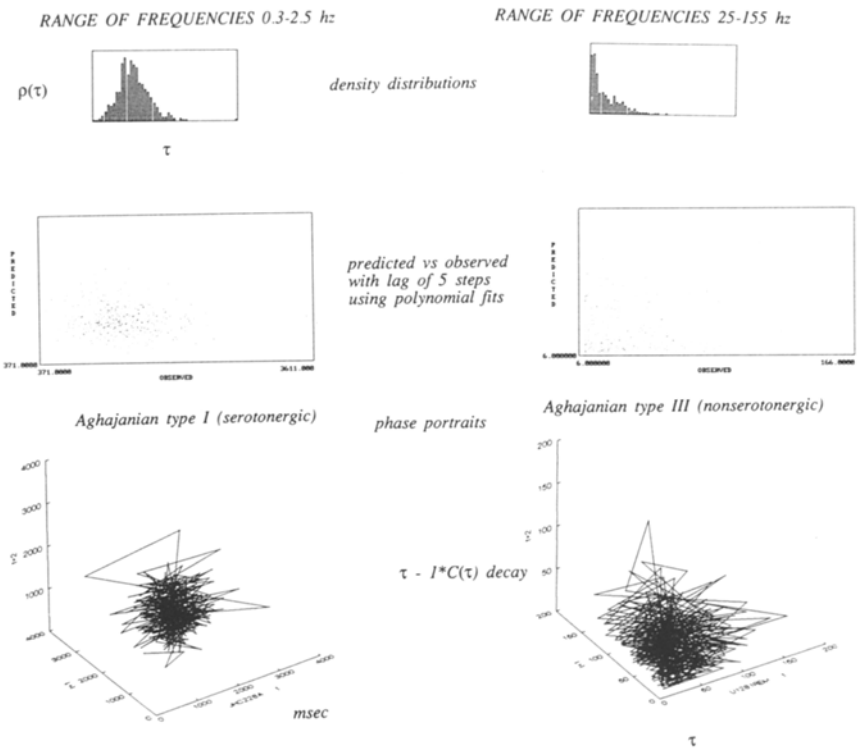

Fig. 7. Slow periodic and fast noise driving of the global membrane brain wave relaxation oscillator. Two neighboring neurons in the dorsal raphe nucleus of the rat whose axons project to the same areas of the neocortex. One is slow and nearly periodic (left), and the other is faster and more irregular. The density distributions, the polynomial predictability, and the three-dimensional phase portrait of the interspike interval time series from each cell describe these properties. (Data of JoAnn Carlsson, Stephen Foote, Bernat Kocsis and Robert Vertes.)

individual dorsal raphe neuron noise source and that of the global brain wave neuronal membrane subjected to the influence of brain stem driving. We support this conjecture with the arguments presented here and the many classical experiments demonstrating the loss of the normal EEG modes and failures in attentional tasks with brain stem damage, and the temporary reversal of these deficits with noise-simulating electrical stimulation.[29,50]

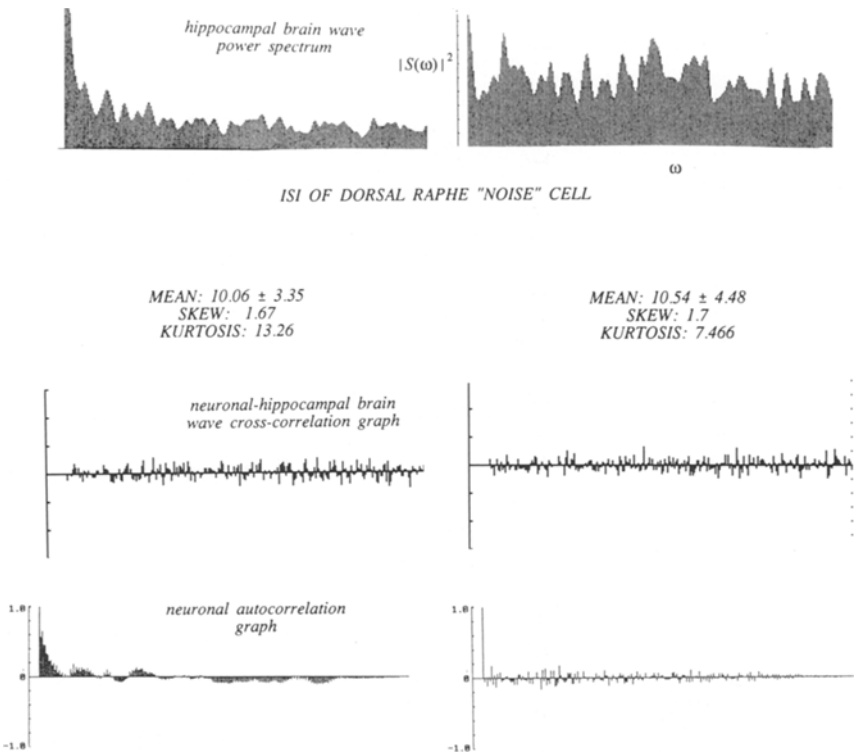

Fig. 8. An example of brain stem noise selection/stabilization of patterns in brain wave modes? Changes in the autocorrelation graph of the time series of interspike intervals of a dorsal raphe fast noise cell is associated with a change in the power spectrum of the EEG as recorded from the rat hippocampus to which it projects. The rat is in (nondreaming) sleep during the left recording, awake in the right recording. Note that whereas there is not a significant difference in the mean and second moment of the interspike intervals between these two states, the fourth moment difference is consistent with the change in the autocorrelation graph. Note also that the cross-correlation of the time series of the brain stem neuron interspike interval and hippocampal (digitized) brain wave signals did not change. (Data of Bernat Kocsis and Robert Vertes.)

ACKNOWLEDGMENTS

We express our appreciation to JoAnn Carlsson, Stephen Foote, Bernat Kocsis, Robert Vertes, and Wally Pritchard for the single neuron and EEG data used in this development. This work was supported by the Office of Naval Research, Systems Biophysics and Cognitive and Neurosciences.

REFERENCES

1. K. A. Selz and A. J. Mandell, Bernoulli partition-equivalence of intermittent neuronal discharge patterns, *Int. J. Bif. Chaos* **1**:717–722 (1991).
2. S. L. Foote and J. H. Morrison, Extrathalamic modulation of cortical function, *Annu. Rev. Neurosci.* **10**:67–95 (1987).
3. A. J. Mandell and K. A. Selz, Period adding, hierarchical protein modes and electroencephalographically defined states of consciousness, in *First Experimental Chaos Conference*, S. Vohra, M. Spano, M. Shlesinger, L. Pecora, and W. Ditto, eds. (World Scientific, Singapore, 1992).
4. A. J. Mandell, K. A. Selz, and M. F. Shlesinger, Some comments on the weaving of contemporary minds; resonant neuronal quasiperiodicity, period adding, and $O(2)$ symmetry in the EEG, in *Measuring Chaos in the Human Brain*, D. Duke and W. Pritchard, eds. (World Scientific, Singapore, 1991).
5. A. Bulsara, E. W. Jacobs, T. Zhou, F. Moss, and L. Kiss, Stochastic resonance in a single neuron model: Theory and analog simulation, *J. Theor. Biol.* **152**:531–555 (1991).
6. A. Longtin, A. Bulsara, and F. Moss, Time-interval sequences in bistable systems and the noise-induced transmission of information by sensory neurons, *Phys. Rev. Lett.* **67**:656–659 (1991).
7. M. P. Paulus, S. F. Gass, and A. J. Mandell, A realistic, minimal "middle layer" for neural networks, *Physica D* **40**:135–155 (1989).
8. E. D. Adrian, F. Bremer, and H. H. Jasper, *Brain Mechanisms and Consciousness* (Thomas, Springfield, Illinois, 1954).
9. J. L. Cummings, *Subcortical Dementia* (Oxford University Press, Oxford, 1990).
10. A. J. Mandell and M. F. Shlesinger, Lost choices; parallelism and topological entropy decrements in neurobiological aging, in *The Ubiguity of Chaos* (AAAS Press, Washington, D.C., 1990).
11. W. S. McCulloch and W. Pitts, A logical calculus of the ideas immanent in nervous activity, *Bull. Math. Biophys.* **5**:115–133 (1943).
12. D. Colquhoun and F. Sigworth, Fitting and statistical analysis of single-channel records, in *Single Channel Recording*, B. Sakmann and E. Neher, eds. (Plenum Press, New York, 1983).
13. L. S. Liebovitch, Testing fractal and Markov models of ion channel kinetics, *Biophys. J.* **55**:373–377 (1989).
14. M. F. Shlesinger, Fractal time in condensed matter physics, *Annu. Rev. Phys. Chem.* **39**:269–290 (1988).
15. A. J. Mandell, From intermittency to transitivity in neuropsychobiological flows, *Am. J. Physiol.* **245**:R484–R494 (1983).
16. A. J. Mandell and J. A. S. Kelso, Dissipative and statistical mechanics of amine neuron activity, in *Essays on Classical and Quantum Dynamics*, J. A. Ellison and H. Uberall, eds. (Gordon and Breach, Philadelphia, 1991).

17. A. J. Mandell and K. A. Selz, Is the EEG a strange attractor? Brain stem neuronal discharge patterns and electroencephalographic rhythms, in *The Impact of Chaos on Science and Society*, C. Grebogi and J. Yorke, eds. (United Nations Press, Tokyo, 1992).
18. M. Levi, Qualitative analysis of the periodically forced relaxation oscillations, *AMS Mem.* #244 (1981).
19. J. P. Eckmann and D. Ruelle, Ergodic theory of chaos and strange attractors, *Rev. Mod. Phys.* **57**:617–656 (1985).
20. K. P. Scholz and J. H. Byrne, Intercellular injection of cyclic AMP induces a long-term reduction of neuronal potassium current, *Science* **240**:1664–1666 (1987).
21. J. P. Keener, Analog circuitry for the van der Pol and FitzHugh–Nagumo equations, *IEEE* **SMC-13**:1010–1014 (1983).
22. J. Grasman, E. J. Veling, and G. M. Willems, Relaxation oscillations governed by a van der Pol equation with periodic forcing term, *SIAM J. Appl. Math.* **31**:667–676 (1976).
23. M. Steriade and R. W. McCarley, *Brain Stem Control of Wakefulness and Sleep* (Plenum Press, New York, 1990).
24. W. R. Klemm and R. P. Vertes, *Brainstem Mechanisms of Behavior* (Wiley, New York, 1990).
25. W. G. Walter, *The Living Brain* (Norton, New York, 1953).
26. L. S. Young, Stochastic stability of hyperbolic attractors, *Ergodic Theory Dynamic Syst.* **6**:311–319 (1986).
27. Y. Kifer, *Random Perturbations of Dynamical Systems* (Birkhauser, Boston, 1988).
28. D. Ruelle, *Chaotic Evolution and Strange Attractors* (Cambridge University Press, Cambridge, 1989).
29. E. D. Adrian, F. Bremer, and H. H. Jasper, *Brain Mechanisms and Consciousness* (Thomas, Springfield, Illinois, 1954).
30. I. Kan and J. A. Yorke, Antimonotonicity: Concurrent creation and annihilation of periodic orbits, *Bull. Am. Math. Soc.* **23**:469–476 (1990).
31. D. Ruelle, Small random perturbations of dynamical systems and the definition of attractors, *Commun. Math. Phys.* **82**:137–151 (1981).
32. F. Moss and P. V. E. McClintock, *Noise in Nonlinear Dynamical Systems* (Cambridge University Press, Cambridge, 1989).
33. E. D. Adrian and B. H. C. Matthews, The Berger rhythm: Potential changes from the occipital lobes in man, *Brain* **57**:355–384 (1934).
34. E. Basar, *EEG-Brain Dynamics* (Elsevier/North-Holland, Amsterdam, 1980).
35. J. P. Crutchfield and B. A. Huberman, Fluctuations and the onset of chaos, *Phys. Lett.* **77A**:407–410 (1980).
36. C. Shagass, Electrical activity of the brain, in *Psychophysiology*, N. S. Greenfield and R. Sternbach, eds. (Holt, Rinehart, and Winston, New York, 1972).
37. A. Babloyantz and A. Dextexhe, Low dimensional chaos in an instance of epilepsy, *Proc. Natl. Acad. Sci. USA* **83**:3513–3517 (1986).
38. A. Babloyantz, J. M. Salazar, and C. Nicolis, Evidence of chaotic dynamics of brain activity during the sleep cycle, *Phys. Lett.* **111A**:152–156 (1985).
39. D. Gallez and A. Babloyantz, Lyapounov exponents for nonuniform attractors, Preprint (1991).
40. P. E. Rapp, Chaos in the neurosciences: Cautionary tales from the frontier, Preprint (1992).
41. C. Grebogi, E. Ott, S. Pelikans, and J. A. Yorke, Strange attractors that are not chaotic, *Physica* **13D**:261–268 (1984).
42. F. J. Romeiras and E. Ott, Strange nonchaotic attractors of the damped pendulum with quasiperiodic forcing, *Phys. Rev. A* **35**:4404–4411 (1987).

43. W. L. Ditto, M. L. Spano, H. T. Savage, S. N. Rauseo, J. Heagy, and E. Ott, Experimental observations of a strange nonchaotic attractor, *Phys. Rev. Lett.* **65**:533–536 (1990).
44. A. Wolf, J. B. Swift, H. L. Swinney, and J. A. Vastano, Determining Lyapounov exponents from a time series, *Physica* **16D**:285–317 (1985).
45. P. E. Rapp, T. R. Bashore, J. M. Martinerie, A. M. Albano, I. D. Zimmerman, and A. I. Mees, Dynamics of brain electrical activity, *Brain Topography* **2**:99–118 (1989).
46. J. Heagy and W. L. Ditto, Dynamics of a two-frequency parametrically driven Duffing oscillator, *J. Nonlinear Sci.* **1**:423–455 (1991).
47. A. I. Mees and P. E. Rapp, Identifying state space dimension from outputs of nonlinear systems, Preprint (1990).
48. G. K. Aghajanian, R. Y. Wang, and J. Baraban, Serotonergic and nonserotonergic neurons of the dorsal raphe, *Brain Res.* **153**:169–175 (1978).
49. R. Vertes, A PHA-L analysis of ascending projections of dorsal raphe nucleus in rat, *J. Comp. Neurol.* **313**:643–668 (1992).
50. J. M. Fuster and R. F. Doctor, Variations of optic lobe evoked potentials as a function of reticular activity in rabbits with implanted electrodes, *J. Neurophysiol.* **25**:324–336 (1962).